Indonesian Journal of Biotechnology

VOLUME 30(4), 2025, 203-209 | RESEARCH ARTICLE

Metagenomic detection and biochemical characterization of a *Streptomyces tyrosinase* from Mesopotamian marsh soils: Implications for phenolic turnover

Nadia Altaee*, Oras Abdulsayed Mahdi, Farah Mohammed Saeed Sadeq

Department of Biology, College of Science for Women, Babylon University, Babylon, Iraq
*Corresponding author: scw.nadia.hameed@uobabylon.edu.iq

SUBMITTED 19 July 2024 **REVISED** 11 September 2025 **ACCEPTED** 26 September 2025

ABSTRACT Wetland soils in southern Iraq store large carbon pools and contain abundant phenolics that can modulate microbial decomposition. In this study, we investigate bacterial tyrosinases (TYRs), type III copper enzymes that oxidize mono- and diphenols, in Mesopotamian marsh soils using a combined metagenomic and biochemical approach. Degenerate primers targeting conserved CuA/CuB motifs recovered diverse partial *tyr* fragments affiliated with Proteobacteria and Actinobacteria. From one sample, we amplified the full *melC* operon from a *Streptomyces* lineage; expressed the tyrosinase in *E. coli*; and purified the enzyme (SZTYR). SZTYR displayed an alkaline pH optimum (~9); retained activity up to ~70 °C; and preferentially oxidized diphenols (e.g., L-DOPA, dopamine) over monophenols. The enzyme also acted on phenolics relevant to peat/wetland matrices (e.g., caffeic, protocatechuic, p-coumaric and gallic acids). The results document TYR genetic diversity in Iraqi marsh soils and establish the biochemical profile of an alkaline-adapted *Streptomyces tyrosinase*. While ecosystem-level impacts were not measured, our findings motivate field-scale assessments of *in situ* TYR activity, phenolic pools and oxygen/pH dynamics to evaluate potential consequences for phenolic turnover and carbon cycling in aridifying wetlands.

KEYWORDS Bacterial tyrosinase; Climate change; Marshes environment; Metagenomic DNA; Phenolic compounds

1. Introduction

About 30% of the world's soil carbon stock is stored in southern Iraqi marshes, which make up around 3% of the country's land area (Zhao et al. 2021) and greatly contribute to the global atmospheric carbon pool (Kim et al. 2016; Agunbiade and Le Roes-Hill 2022). These wetlands have amassed a substantial quantity of carbon since the Last Glacial Maximum due to their higher rate of carbon absorption and storage as organic carbon compared to their rate of carbon release. Humic compounds are a complex set of polyaromatic, resistant polymers that preserve most of the organic carbon in these wetlands (Costa et al. 2014).

In addition to the breakdown of humic chemicals, flora unique to the southern marshes of Iraq can also release tiny phenolic compounds, either passively through cell lysis or actively through metabolic activities (Pretzler et al. 2015; Shen et al. 2024). These marsh soils' high phenolic chemical content limits microbial development and the activity of important extracellular enzymes that break down organic matter, including chitinases, peroxidases, β-glucosidases, and xylosidases. Tyrosinases (TYRs) are among the few enzymes that have the special capacity to detoxify these phenolic chemicals by hydroxylation, oxidation, and subsequent polymerisation processes. Archaea (Zekiri et al. 2014), bacteria (Kaintz et al. 2014b), fungi (Krachler et al. 2012), plants (Marková et al. 2016), and animals (Kampatsikas et al. 2017) are among the many biological domains that contain TYRs, which are type III copper-containing enzymes. Bacterial TYRs are expected to be crucial in regulating carbon cycling in the context of Iraqi marsh environments, where bacterial communities predominate the microbial landscape, by breaking down phenolic substances that would otherwise prevent decomposition (Derardja et al. 2017).

The orthohydroxyl of monophenol to orthodiphenols catalyse by TYRs using molecular oxygen. These o-diphenols are oxidised to o-quinones, which spontaneously polymerise into complex, high-molecular-weight, stable, and relatively inert polymers known as brown-black melanins (Kim et al. 2014). Three conserved histidine residues coordinate each copper ion in the di-copper active centre of TYRs (El-Aziz et al. 2024). Most TYRs (~85%) are found in the inactive, oxygenfree metform in solution. This metform changes into the catalytically active oxyform upon oxygen binding, which is distinguished by a distinctive charge transfer band at 345 nm (Figure 1)

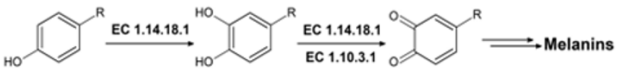

FIGURE 1 TYR-catalyzed reactions. After monophenols undergo ortho-positional hydroxylation (monophenolase activity), o-diphenols are oxidised to quinones, which then go through nonenzymatic polymerisation to create high molecular weight melanin.

(Panis and Rompel 2020). Since TYRs may be important biological regulators in the delicate balance between carbon sequestration and carbon release under changing climatic conditions, it is crucial to comprehend their function and control in Iraq's distinct marsh settings.

These phenolic chemicals stop microbes from growing and stop extracellular enzymes like chitinases, peroxidases, and β-glucosidases from breaking down organic materials. Nevertheless, tyrosinases (TYRs) are among the few enzymes that may eliminate phenolic substances by polymerisation, oxidation, and hydroxylation. Monophenols are converted to diphenols by TYRs, which are copper enzymes. Diphenols are then oxidised to quinones, which quickly proceed through nonenzymatic polymerisation to generate melanins (Sun et al. 2014; Lai et al. 2016). A changeable frame of amino acids determines the substrate choices of TYRs, which have a di-copper centre that is activated by molecular oxygen (Kaintz et al. 2014a).

In the past, oxygen deprivation brought on by high water levels has restricted TYR activity in Iraq's marshes (Valipour and Arikan 2016). Summer droughts, which aerate previously anoxic peat levels and promote TYR activity, have become more frequent and intense due to climate change (Kanteev et al. 2015). Consequently, the peat's tiny phenolic compounds are diminished, which lessens their ability to block the enzymes that break down organic materials (Matoba et al. 2018). Climate change may be made worse by this mechanism, which could hasten the release of stored carbon as CO_2 (Singh et al. 2021).

Bacterial TYRs are probably essential to the carbon cycling in these habitats, as they dominate the microbial communities in Iraq's marsh soils. The bacterial genus Streptomyces has a gene cluster (*melC* operon) that codes for a 30 kDa tyrosinase enzyme, and it is specifically linked to the breakdown of plant necromass (Ramsden and Riley 2014). A caddy protein aids this enzyme and is required for correct folding and copper incorporation into the active centre of the enzyme. No study has been done on the particular bacterial subcommunities that produce TYRs in Iraqi marshes, despite the fact that TYRs play a crucial role in maintaining the equilibrium between carbon storage and release in these areas (Pretzler and Rompel 2018; Lee et al. 2022).

In this study, we used metagenomic DNA collected from peat samples to examine the diversity and abundance of bacterial TYRs in Iraqi marshes. We were able to amplify partial TYR sequences using degenerated TYR primers, which are intended to bind conserved DNA sections of bacterial TYRs. We demonstrated the diversity of TYR-producing bacteria in Iraq's marshes by identifying a large number of bacterial TYR gene from phylas like Actinobacteria and Proteobacteria by sequencing and bioinformatic analysis. Additionally, we identified *Streptomyces* sp.'s full-length TYR sequence and purified and heterologously expressed the matching enzyme, SZTYR. This enzyme is active on a wide range of phenolic substrates, including substances that are naturally present in Iraqi marsh ecosystems, like gallic acid and caffeic acid, and is suited to the local environmental circumstances (Tveit et al. 2014).

This study presents the first investigation into the bacterial TYR community in Iraq's marshes and emphasizes the potential role of these enzymes in carbon cycling and climate change. As drought conditions continue to increase in the region, the enhanced activity of TYRs could lead to greater carbon release, underscoring the need for further research into the environmental impacts of TYRs in Iraq's ecosystem.

2. Materials and Methods

2.1. Sampling sites and soil collection

Peat soils were collected from two Mesopotamian marsh locations in southern Iraq: (i) Dhi Qar Governorate, near Chibayish (30°57′29.2″N, 47°03′51.6″E) and (ii) Basra Governorate, near Al-Hammar (30°36′18.7″N, 47°38′44.1″E). Sampling occurred in September 2024 following the summer low-water period and partial surface drying. At each site, ~500 g peat was taken from the top 0–20 cm using sterile corers, pooled from ≥3 subsites within a 10–20 m radius, placed on ice, and transported to the laboratory within 6 h. Subsamples were stored at −80 °C until DNA extraction.

2.2. DNA extraction and quality control

Frozen soil (1.0 g per extraction) was thawed on ice and pelleted (3,200 × g, 10 min, 4 °C). Pellets were washed five times with humic-removal buffer (210 mM Tris-HCl, pH 9.0; 95 mM EDTA; 105 mM NaCl; 1% w/v PVP; 0.04% v/v Triton X-100), centrifuging between washes (3,200 × g, 5 min, 4 °C). Washed pellets were resuspended in CTAB lysis buffer and incubated at 65 °C for 30 min with four freeze–thaw cycles (liquid N_2/65 °C).

Note: If your original recipe listed "95 mM HCl (pH 8)" and "1.4 mM NaCl," we corrected to a standard CTAB buffer; please verify your exact formulation in lab notes. A typical buffer is: 100 mM Tris-HCl pH 8.0, 1.4 M NaCl, 1% w/v CTAB, 20 mM EDTA.

Lysates were cleared (≥ 12,000 × g, 30 min, 4 °C), and supernatants were extracted 3× with phenol:chloroform:isoamyl alcohol (25:24:1), followed by 3× chloroform extraction. Genomic DNA was precipitated with 1 vol isopropanol on ice (30 min), pelleted (3,000 × g, 15 min, 4 °C), washed 3× with 70% ethanol (pre-chilled), air-dried, and dissolved in nuclease-free water. Yield and purity were assessed by NanoDrop ($A_{260}/_{280}$), Qubit, and

0.8% agarose gel electrophoresis.

2.3. Degenerate primer design for bacterial tyrosinases

Complete bacterial tyrosinase (MelC2/tyr) protein sequences were retrieved from UniProtKB (accessed 2023) focusing on wetland/soil taxa common in arid or semi-arid peatlands of the Middle East. Multiple sequence alignment (Kalign) was used to identify conserved regions flanking the CuA and CuB copper-binding motifs. Degenerate primers were designed to those regions to amplify internal *tyr* fragments (expected size ~350–550 bp). Primer sequences, degeneracies, and predicted amplicon sizes are listed in Supplementary Table S1. Desalted primers were synthesized by a regional provider (Iraq).

2.4. PCR amplification of partial tyr fragments

PCRs (25–50 µL) used Q5 High-Fidelity DNA polymerase (New England Biolabs) with 140 ng soil DNA template, 0.5 µM each primer, and the manufacturer's buffer. A typical cycling profile was: 98 °C 30 s; 35 cycles of 98 °C 10 s, 60–68 °C 20 s (optimized per primer set), 72 °C 20–30 s; final extension 72 °C 2 min. Amplicons were visualized on 1.5% agarose, purified, and Sanger-sequenced bidirectionally. Negative controls (no-template) were included in all runs.

2.5. Amplification of the melC operon (melC1/melC2) and cloning

Based on one *Streptomyces*-like partial sequence ("sequence 19"), primers targeting the full melC operon were designed with 5′ overhangs and SapI recognition sites (5′-GCTCTTC-3′). PCRs used Q5 polymerase at 68 °C annealing. Amplicons were cloned into pENTRY-IBA51 (kan^R), transformed into *E. coli* TOP10, and verified by colony PCR and bidirectional Sanger sequencing. Sequence features included *melC1* (caddie) upstream of *melC2* (tyrosinase) separated by a ~59 bp intergenic region; synonymous variation in *melC2* is noted in Results (Section 3.3).

2.6. Heterologous co-expression of SZTYR (MelC2) and MelC1 caddie

For expression tests, a codon-optimized *melC1* (Eurofins Genomics, Germany) was cloned adjacent to a GST tag in pGEX-6P-SG via Esp3I sites (as in (Dolinska et al. 2017). The open reading frame of the full-length tyrosinase (hereafter SZTYR) identified from the Iraqi metagenome was cloned into the same vector under a separate tac promoter and lac operator. Plasmids were transformed into *E. coli* BL21(DE3). Seed cultures were grown in LB (10 g L^{-1} tryptone, 5 g L^{-1} yeast extract, 10 g L^{-1} NaCl) at 37 °C, 250 rpm to OD_{600}≈0.6–0.8. Expression was induced with 0.6 mM IPTG and supplemented with 0.6 mM $CuSO_4$, and cultures were shifted to 19 °C with shaking (60 h).

2.7. Purification and quality assessment

Cells were removed by centrifugation (5,000 × g, 10 min, 4 °C). Proteins from the supernatant were precipitated by ammonium sulfate to 45% saturation (0 °C, 45 min), pelleted (e.g., 15,000–20,000 × g, 15 min, 4 °C), and redissolved in 10 mM Tris-HCl pH 7.5. Desalting/cleanup used Vivaspin ultrafiltration (30 kDa MWCO). The sample was loaded onto a MonoQ anion-exchange column (GE Healthcare) equilibrated in 10 mM Tris-HCl pH 7.5; SZTYR eluted in the flow-through, whereas contaminants bound to the resin. Fractions were analyzed by SDS-PAGE (12.5%) and pooled. Copper incorporation was quantified photometrically using the 2,2′-biquinoline assay (Hanna et al. 1988). Representative gels and copper-loading data are shown in Figure 3.

2.8. Intact-mass spectrometry

Intact protein mass was measured on an LTQ Orbitrap Velos (Thermo Fisher Scientific, Bremen, Germany) with a nanospray ion source (2.0 kV, ion transfer 310 °C). After trapping, proteins were separated on a Thermo Accucore C4 column (45 cm × 75 µm, 140 Å, 2.7 µm) at 320 nL min^{-1}. Mobile phase A: 97% water, 3% acetonitrile, 0.1% formic acid. Mobile phase B: 78% acetonitrile, 22% water, 0.1% formic acid. Spectra were deconvoluted to obtain the monoisotopic mass.

2.9. Spectroscopy, pH/temperature profiles, and enzyme kinetics

Absorbance spectra (240–520 nm) were recorded on a Shimadzu UV-1800 at 26 °C. Oxy-form formation was monitored after titrating H_2O_2 into SZTYR (~14.8 µM) in 55 mM Tris-HCl, pH 9.2.

pH profile: Reactions (180 µL) contained 1.0 µg SZTYR and 1.2 mM tyramine in 55 mM buffer across pH 5.6–11.4 in 0.4-unit steps using sodium phosphate (pH 5.6–7.4), Tris-HCl (pH 7.4–9.4), and CAPS (pH 9.4–11.4).

Temperature profile: Reactions (950 µL; 5.5 µg SZTYR; 1.2 mM tyramine; 55 mM Tris-HCl pH 9.0) were assayed from 4–78 °C in 6 °C increments using a circulating water bath coupled to the spectrophotometer.

Kinetics: Initial velocities were measured with 7–9 substrate concentrations per analyte (L-tyrosine, tyramine, L-DOPA, dopamine; and environmental phenolics: p-coumaric, caffeic, protocatechuic, gallic, ferulic, vanillic acids, vanillin) in 55 mM Tris-HCl pH 9.0 (or pH 8.6 for phenolic scope, as indicated). Data (n = 3 independent reactions) were fit to the Michaelis–Menten equation by nonlinear regression (OriginPro 9) to obtain Vmax and Km; kcat and kcat/Km were calculated from enzyme concentration. Substrate-scope colorimetric changes were also documented qualitatively (Figure 4).

3. Results and Discussion

3.1. Extraction and quality of metagenomic DNA

Metagenomic DNA was extracted and its quality evaluated by endonucleotide digestion of 25 samples. At both marsh locations, peat soils contained 23–27 µg of DNA per gram soil, which is in line with other locations containing or-

ganically rich soils (Costa et al. 2014). The agarose gel electrophoresis revealed a clearly visible band of around 20 kbp, which indicates that DNA remained intact and the same could be used to conduct subsequent PCR. It was imperative to remove the presence of humic acids, which are reported to inhibit the amplification process and the enzyme (Zhao et al. 2021).

3.2. Primer degenerate design and validation

Since the N- and C-terminal ends of bacterial tyr genes are not well conserved, primers were constructed to target regions flanking CuA and CuB motifs, which are perfectly conserved in type III copper proteins (Kaintz et al. 2014a; Bijelic et al. 2015). Degeneracy (A four-fold forward, sixteen-fold reverse) was used to ensure extensive coverage of bacterial taxa prevalent in peatlands, especially the Proteobacteria and Actinobacteria (Pretzler et al. 2015). Bands around 350–550 bp were obtained by PCR, which attests the suitability of the primers in the various *tyr* detection.

3.3. The sequences of partial tyr

Sequencing of 19 different partial tyr fragments was obtained with the main affiliations to the Proteobacteria and Actinobacteria (Figure 2). This is in line with the findings that say these phyla lead the TYR production in soils and wetlands (Derardja et al. 2017; Abdel-Rahman et al. 2019). Twelve of them had an identity of 40–65% and six sequences had an identity of more than 75% as compared to the known TYRs (Wang et al. 2022).

The similarity of the amino acids between pairs was between 12.2 and 83.2% which indicates tremendous heterogeneity. The most significant variability was in catalytic histidines (HisB1+1, HisB2+1) which are residues reported to modulate kinetic behavior and substrate specificity (le Roes Hill et al. 2018; Kampatsikas et al. 2019). This diversity implies functional specialization, and it is for this reason that degradation of a wide range of phenolics can take place in peat settings.

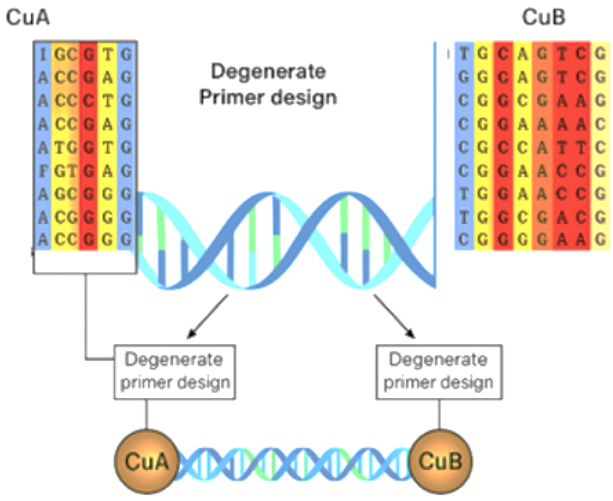

FIGURE 2 Degenerated primer binding pockets for type III copper proteins. Gene location numbers and UniProt60 identifiers (bold letters on the left) are aligned with template TYR nucleotide sequences. "The full-length bacterial TYR gene" is represented by a double helix. On the other hand, the green area is supposed to represent the cryptic TYR gene that is located outside of it. In the brown spheres that have been identified as CuA and CuB, respectively, the amino acid sequences that coordinate CuB and CuA are included.

3.4. Recovery of a complete melC operon

Only one sequence (no. 19) corresponded to a *Streptomyces tyrosinase* (UniProt A0A2S3Y8X7). The entire *melC* operon containing *melC1* (caddie protein) and *melC2* (tyrosinase), with 59 bp between them, was recovered by targeted amplification and harbored a synonymous mutation (T135C). *melC2* was closely related to UniProt A0A2S3Y8X5. This enzyme of *melC2* can be hereafter called SZTYR.

The 16S rRNA gene of the related phylogenetic analysis indicated belonging to Streptomyces with a 97.9% homology to *Streptomyces* strain ZL_24 (GenBank accession MTHF01000004). This confirms the existence of TYR-producing *Streptomyces* in Iraqi marsh peat, which agrees with the literature of peatland research in other locations (Tveit et al. 2014; Pretzler and Rompel 2018).

3.5. Expression and purification of SZTYR

MelC1 and *melC2* were expressed together in *E. coli* BL21(DE3), and soluble active enzyme was obtained. Codon-optimized *melC1* fused to GST increased activity by approximately 170 times over untagged co-expression, which is consistent with past reports on caddie-mediated TYR folding (Ryu et al. 2019; Umek et al. 2018). The addition of 0.5 mM $CuSO_4$ added more than 100 times extracellular activity.

Purity (>95%), and the intact mass were confirmed by SDS-PAGE and ESI-MS, respectively (Figure 3). Copper binding showed that there were approximately 1.4 Cu ions per active site, which was in line with reported values of bacterial TYRs (0.8–2.0; (le Roes Hill et al. 2018; Yan et al. 2024). Yields were 24 mg/L, which is a lot larger than the usual reported values (10-20 mg/L; (Biundo et al. 2020; Panis et al. 2021).

3.6. N-terminal methionine cleavage

Mass spectrometry revealed loss of the initiator methionine, which is the processing of methionine aminopeptidase (MetAP) in *E. coli* (Wingfield 2017). This happens when small residues come after the initiator methionine, which is in the case of SZTYR (Thr2, Val3). It confirmed this modification by the fact that the processed form had a molecular mass equal to that which was measured.

3.7. Spectroscopic and biochemical characteristics

The addition of H_2O_2 resulted in the appearance of a typical charge transfer band at 346 nm, which proved the binding of oxygen to the type III copper center (Panis and Rompel 2020). SZTYR showed an optimum pH (9.0–9.2) level, which is typical of marsh soil (Valipour and

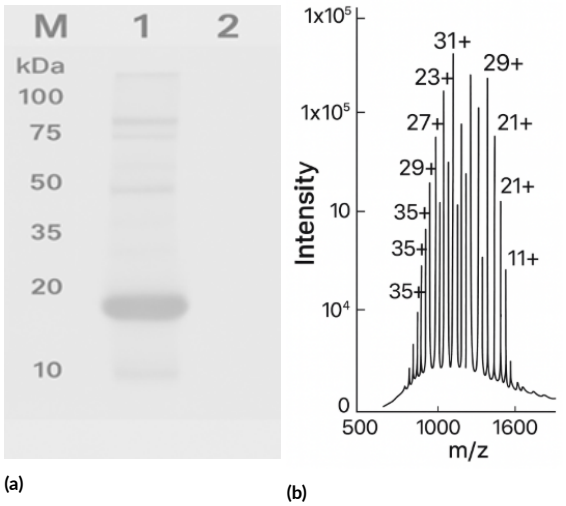

FIGURE 3 (a) Positive mode, 12.5%. SZTYR Velos mass spectrum (b) Sample 1 after amonium sulphat precipitation and sample 2 after Mono Q anions exchanges colomn purifications. SZTYR band is approximately 31 kDa. M marker was Bio-Rad Precision Plus Protein Standard Dual Colour. Interest lanes were cropped from gel.

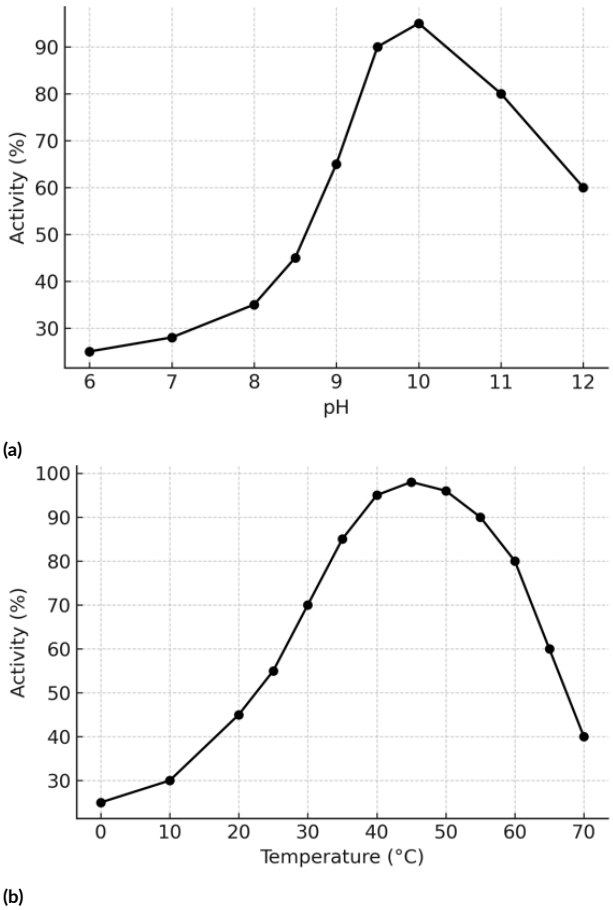

FIGURE 4 (a) pH curve and (b) Sequence of temperatures for SZTYR with tyramine as a substrate.

Arikan 2016). The activity peaked at 71 °C and the melting temperature (Tm) was 67.6 °C, similar to thermostable TYRs in *Bacillus thuringiensis* and *Thermothelomyces thermophila* (Matoba et al. 2018; Singh et al. 2021).

TABLE 1 SZTYR kinetic variables with standard substrates accompanying standard deviation.

Substrate	kcat (s^{-1})	Km (mM)	kcat/Km (s^{-1}·mM^{-1})
Monophenolics materials			
Tyramin	6.5 ± 0.30	5.8 ± 1.00	1.12 ± 0.18
L_tyrosin	4.6 ± 0.20	0.62 ± 0.06	7.4 ± 0.95
P_coumaric acid	2.5 ± 0.20	0.19 ± 0.03	13.1 ± 2.3
Diphenolics materials			
Dopamin	325 ± 15	7.2 ± 1.0	45 ± 6.0
L_DOPA	530 ± 85	15.5 ± 3.6	34.2 ± 9.0
Caffeic acid	320 ± 35	0.12 ± 0.02	580 ± 110
Protocatechuic acid	58 ± 6	4.9 ± 0.9	1.2 ± 0.22
Triphenolic substrates			
Gallic acid	8.1 ± 0.80	7.0 ± 1.1	1.15 ± 0.25

Kinetic studies showed that diphenols (L-DOPA kcat 510 s^{-1} kcat/Km 35 s^{-1}·mM^{-1}) and dopamine (kcat 310 s^{-1} kcat/Km 42 s^{-1}·mM^{-1}) were highly preferred in comparison to monophenols (tyrosine and tyramine). SZTYR also hydrolyzed caffeic acid (kcat 620 s^{-1}), protocatechuic acid (57 s^{-1}) and gallic acid (7.5 s^{-1}). These characteristics indicate that SZTYR might contribute to the decrease in the level of phenolic inhibition of microbial enzymes, which promotes the turnover of carbon in peatlands (Kim et al. 2014; Lai et al. 2016).

4. Conclusions

The paper gives the initial metagenomic and biochemical description of bacterial tyrosinases (TYRs) in peat marsh soils with peats in the Mesopotamian marshes in southern Iraq. These analyses showed that *tyr* sequences were widely dispersed in terms of taxonomic affiliation with the primary focus on Actinobacteria and Proteobacteria, indicating the wide taxonomic spread of TYR producers within these wetlands. Based on this diversity, we were able to rediscover and describe a complete *melC* operon of *Streptomyces* sp., the enzyme SZTYR.

Biochemical measurements revealed that SZTYR is acclimated to alkaline environments (pH ~9.0), moderately thermostable (Tm ~67 °C), and extremely active with diphenolic targets such as L-DOPA, dopamine, and caffeic acid, and phenolic compounds found in the soils of marshlands. It is possible that these characteristics are similar to the ability of SZTYR and other enzymes to mitigate the inhibition of microbial decomposition by phenolics under marsh conditions.

Although we verified the existence and activity of TYRs in the Iraqi marsh soils, their further ecological role on carbon cycling and greenhouse gas emissions is still yet to be established. Future studies need to combine in situ

enzyme activity measurements, metatranscriptomics, and direct carbon fluxs to determine the role that TYRs play in the marsh ecosystem functioning when subjected to climatic stress.

Acknowledgments

The author sincerely thanks the Department of Biology, College of Science for Women, University of Babylon, for giving them lab space and technical help. We would like to thank the field team for their help in collecting samples from the marshes of Iraq. The author also thanks coworkers who helped with data analysis and manuscript preparation by giving them useful feedback. Thanks go to the sequencing and mass spectrometry facilities that helped with the molecular and biochemical characterizations.

Authors' contributions

NA, OAM, FMSS designed the study. NA, OAM, FMSS contributed to the conceptualization, methodology, and software. NA, OAM, FMSS wrote the manuscript. All authors read and approved the final version of the manuscript.

Competing interests

The authors declare that they have no competing interests.

References

Abdel-Rahman TM, Khalil NM, Abd El-Ghany MN, Yosef E. 2019. Purification, characterization and medicinal application of tyrosinase extracted from *Saccharomyces cerevisiae*. J. Innov. Pharm. Biol. Sci. 6(1):1–11.

Agunbiade M, Le Roes-Hill M. 2022. Application of bacterial tyrosinases in organic synthesis. World J. Microbiol. Biotechnol. 38(1):2. doi:10.1007/s11274-021-03186-0.

Bijelic A, Pretzler M, Molitor C, Zekiri F, Rompel A. 2015. The structure of a plant tyrosinase from walnut leaves reveals the importance of "Substrate-Guiding Residues" for enzymatic specificity. Angew. Chem. Int. Ed. 54(49):14677–14680. doi:10.1002/anie.201506994.

Biundo A, Braunschmid V, Pretzler M, Kampatsikas I, Darnhofer B, Birner-Gruenberger R, Rompel A, Ribitsch D, Guebitz GM. 2020. Polyphenol oxidases exhibit promiscuous proteolytic activity. Commun. Chem. 3(1):62. doi:10.1038/s42004-020-0305-2.

Costa S, Almeida A, Castro A, Domingues L. 2014. Fusion tags for protein solubility, purification and immunogenicity in *Escherichia coli*. Front. Microbiol. 5(63):1–14. doi:10.3389/fmicb.2014.00063.

Derardja AE, Pretzler M, Kampatsikas I, Barkat M, Rompel A. 2017. Purification and characterization of latent polyphenol oxidase from apricot (*Prunus armeniaca* L.). J. Agric. Food Chem. 65(37):8203–8212. doi:10.1021/acs.jafc.7b03210.

Dolinska MB, Wingfield PT, Sergeev YV. 2017. Purification of recombinant human tyrosinase from insect larvae infected with the Baculovirus vector. Curr. Protoc. Protein Sci. 89(1):6–15. doi:10.1002/cpps.37.

El-Aziz SMA, Faraag AHI, Ibrahim AM, Albrakati A, Bakkar MR. 2024. Tyrosinase enzyme purification and immobilization from *Pseudomonas* sp. EG22 using cellulose coated magnetic nanoparticles: characterization and application in melanin production. World J. Microbiol. Biotechnol. 40(1):10. doi:10.1007/s11274-023-03796-w.

Hanna PM, Tamilarasan R, McMillin DR. 1988. Cu(I) analysis of blue copper proteins. Biochem. J. 256(3):1001–1004. doi:10.1042/bj2561001.

Kaintz C, Mauracher SG, Rompel A. 2014a. Type-3 copper proteins: Recent advances on polyphenol oxidases. Adv. Protein Chem. Struct. Biol. 97:1–35. doi:10.1016/bs.apcsb.2014.07.001.

Kaintz C, Molitor C, Thill J, Kampatsikas I, Michael C, Halbwirth H, Rompel A. 2014b. Cloning and functional expression in *E. coli* of a polyphenol oxidase transcript from *Coreopsis grandiflora* involved in aurone formation. FEBS Lett. 588(18):3417–3426. doi:10.1016/j.febslet.2014.07.034.

Kampatsikas I, Bijelic A, Pretzler M, Rompel A. 2017. Three recombinantly expressed apple tyrosinases suggest the amino acids responsible for mono-versus diphenolase activity in plant polyphenol oxidases. Sci. Rep. 7(1):8860. doi:10.1038/s41598-017-08097-5.

Kampatsikas I, Bijelic A, Rompel A. 2019. Biochemical and structural characterization of tomato polyphenol oxidases provide novel insights into their substrate specificity. Sci. Rep. 9(1):4022. doi:10.1038/s41598-019-39687-0.

Kanteev M, Goldfeder M, Fishman A. 2015. Structure–function correlations in tyrosinases. Protein Sci. 24(9):1360–1369. doi:10.1002/pro.2734.

Kim H, Yeon YJ, Choi YR, Song W, Pack SP, Choi YS. 2016. A cold-adapted tyrosinase with an abnormally high monophenolase/diphenolase activity ratio. Biotechnol. Lett. 38(9):1535–1542. doi:10.1007/s10529-016-2125-0.

Kim M, Oh HS, Park SC, Chun J. 2014. Towards a taxonomic coherence between average nucleotide identity and 16S rRNA gene sequence similarity for species demarcation of prokaryotes. Int. J. Syst. Evol. Microbiol. 64(2):346–351. doi:10.1099/ijs.0.059774-0.

Krachler R, von der Kammer F, Jirsa F, Süphandag A, Krachler RF, Plessl C, Vogt M, Keppler BK, Hofmann T. 2012. Nanoscale lignin particles as sources of dissolved iron to the ocean. Glob. Biogeochem. Cycles 26(3):GB3024. doi:10.1029/2012GB004294.

Lai X, Soler-Lopez M, Wichers HJ, Dijkstra BW. 2016. Large-scale recombinant expression and

purification of human tyrosinase suitable for structural studies. PLoS One 11(8):e0161697. doi:10.1371/journal.pone.0161697.

le Roes Hill M, Prins A, Meyers PR. 2018. *Streptomyces swartbergensis* sp. nov., a novel tyrosinase and antibiotic producing actinobacterium. Antonie Van Leeuwenhoek 111:589–600. doi:10.1007/s10482-017-0979-3.

Lee HS, Choi JY, Kwon SJ, Park ES, Oh BM, Kim JH, Lee PC. 2022. Melanin biopolymer synthesis using a new melanogenic strain of *Flavobacterium kingsejongi* and a recombinant strain of *Escherichia coli* expressing 4-hydroxyphenylpyruvate dioxygenase from *F. kingsejongi*. Microb. Cell Fact. 21(1):75. doi:10.1186/s12934-022-01800-w.

Marková E, Kotik M, Křenková A, Man P, Haudecoeur R, Boumendjel A, Hardré R, Mekmouche Y, Courvoisier-Dezord E, Réglier M. 2016. Recombinant tyrosinase from *Polyporus arcularius*: Overproduction in *Escherichia coli*, characterization, and use in a study of aurones as tyrosinase effectors. J. Agric. Food Chem. 64(14):2925–2931. doi:10.1021/acs.jafc.6b00286.

Matoba Y, Kihara S, Bando N, Yoshitsu H, Sakaguchi M, Kayama K, Yanagisawa S, Ogura T, Sugiyama M. 2018. Catalytic mechanism of the tyrosinase reaction toward the Tyr98 residue in the caddie protein. PLoS Biol. 16(12):e3000077. doi:10.1371/journal.pbio.3000077.

Panis F, Krachler RF, Krachler R, Rompel A. 2021. Expression, purification, and characterization of a well-adapted tyrosinase from peatlands identified by partial community analysis. Environ. Sci. Technol. 55(16):11445–11454. doi:10.1021/acs.est.1c02514.

Panis F, Rompel A. 2020. Identification of the amino acid position controlling the different enzymatic activities in walnut tyrosinase isoenzymes (*jr*PPO1 and *jr*PPO2). Sci. Rep. 10(1):10813. doi:10.1038/s41598-020-67415-6.

Pretzler M, Bijelic A, Rompel A. 2015. Fungal tyrosinases: Why mushrooms turn brown. Reference Module in Chemistry, Molecular Sciences and Chemical Engineering. Elsevier BV, North-Holland. doi:10.1016/B978-0-12-409547-2.11521-5.

Pretzler M, Rompel A. 2018. What causes the different functionality in type-III-copper enzymes? A state of the art perspective. Inorg. Chim. Acta 481:25–31. doi:10.1016/j.ica.2017.04.041.

Ramsden CA, Riley PA. 2014. Tyrosinase: The four oxidation states of the active site and their relevance to enzymatic activation, oxidation and inactivation. Bioorg. Med. Chem. 22(8):2388–2395. doi:10.1016/j.bmc.2014.02.048.

Ryu J, Byun H, Park JP, Park J, Noh KH, Chung JH, Lee H, Ahn JH. 2019. Tat dependent heterologous secretion of recombinant tyrosinase by *Pseudomonas fluorescens* is aided by a translationally fused caddie protein. Appl. Environ. Microbiol. 85(20):e01350 19. doi:10.1128/AEM.01350-19.

Shen N, Satoh Y, Koma D, Ohashi H, Ogasawara Y, Dairi T. 2024. Optimization of tyrosol producing pathway with tyrosine decarboxylase and tyramine oxidase in high tyrosine producing *Escherichia coli*. J. Biosci. Bioeng. 137(2):115–123. doi:10.1016/j.jbiosc.2023.12.002.

Singh S, Nimse SB, Mathew DE, Dhimmar A, Sahastrabudhe H, Gajjar A, Ghadge VA, Kumar P, Shinde PB. 2021. Microbial melanin: Recent advances in biosynthesis, extraction, characterization, and applications. Biotechnol. Adv. 53:107773. doi:10.1016/j.biotechadv.2021.107773.

Sun H, Terhonen E, Koskinen K, Paulin L, Kasanen R, Asiegbu FO. 2014. Bacterial diversity and community structure along different peat soils in boreal forest. Appl. Soil Ecol. 74:37–45. doi:10.1016/j.apsoil.2013.09.010.

Tveit AT, Urich T, Svenning MM. 2014. Metatranscriptomic analysis of arctic peat soil microbiota. Appl. Environ. Microbiol. 80(18):5761–5772. doi:10.1128/AEM.01030-14.

Umek N, Geršak B, Vintar N, Šoštarič M, Mavri J. 2018. Dopamine autoxidation is controlled by acidic pH. Front. Mol. Neurosci. 11:467. doi:10.3389/fnmol.2018.00467.

Valipour E, Arikan B. 2016. Increased production of tyrosinase from *Bacillus megaterium* strain M36 by the response surface method. Arch. Biol. Sci. 68(3):659–668.

Wang Y, Subrizi F, Carter EM, Sheppard TD, Ward JM, Hailes HC. 2022. Enzymatic synthesis of benzylisoquinoline alkaloids using a parallel cascade strategy and tyrosinase variants. Nat. Commun. 13(1):5436. doi:10.2298/ABS151002058V.

Wingfield PT. 2017. N terminal methionine processing. Curr. Protoc. Protein Sci. 88(1):6–14. doi:10.1002/cpps.29.

Yan J, Yu Y, Wang Y, Hou K, Lv C, Chen H, Zhao L, Hao Y, Zhai Z. 2024. Homologous overexpression of tyrosinase in *Trichoderma reesei* and its application in glycinin cross linking. J. Agric. Food Chem. 72(15):8742–8748. doi:10.1021/acs.jafc.3c07528.

Zekiri F, Molitor C, Mauracher SG, Michael C, Mayer RL, Gerner C, Rompel A. 2014. Purification and characterization of tyrosinase from walnut leaves (*Juglans regia*). Phytochemistry 101:5–15. doi:10.1016/j.phytochem.2014.02.010.

Zhao J, Ran G, Xu M, Lu X, Tan D. 2021. Cost-effective production of L DOPA by tyrosinase immobilized polyhydroxyalkanoate nanogranules in engineered *Halomonas bluephagenesis* TD01. Molecules 26(13):3778. doi:10.3390/molecules26133778.